Journal of Molecular Structure 1111 (2016) 84–89

Contents lists available at ScienceDirect

Journal of Molecular Structure

journal homepage: http://www.elsevier.com/locate/molstruc

Ruthenium(III)/phosphine/pyridine complexes applied in the hydrogenation reactions of polar and apolar double bonds

Claudia Rodrigues [a, 1], Fábio G. Delolo [a], Lucas M. Ferreira [a], Pedro I. da S. Maia [b], Victor M. Deflon [b], Jabor Rabeah [c], Angelika Brückner [c], Jakob Norinder [c], Armin Börner [c], André L. Bogado [d, **], Alzir A. Batista [a, *]

[a] Departamento de Química, Universidade Federal de São Carlos, Rod. Washington Luís, km 235 – SP-310, CEP 13565-905 São Carlos, SP, Brazil
[b] Instituto de Química de São Carlos, Universidade de São Paulo, Av. Trabalhador São-carlense, 400, CEP 13566-590 São Carlos, SP, Brazil
[c] Leibniz-Institut für Katalyse an der Universität Rostock e.V., A.-Einstein-Str. 29a, 18059 Rostock, Germany
[d] Faculdade de Ciências Integradas do Pontal, Universidade Federal de Uberlândia, Rua vinte, 1600, CEP 38304-402 Ituiutaba, MG, Brazil

ARTICLE INFO

Article history:
Received 3 November 2015
Received in revised form
27 January 2016
Accepted 28 January 2016
Available online 29 January 2016

Keywords:
Ruthenium(III) complexes
Phosphine-pyridine ligands
Homogeneous catalysis
Hydrogenation reactions

ABSTRACT

In this work, five ruthenium(III) complexes containing phosphine and pyridine based ligands with general formula *mer*-[$RuCl_3$(dppb)(N)] [where dppb = 1,4-bis(diphenylphosphino)butane and N = pyridine (py), 4-methylpyridine (4-Mepy), 4-vinylpyridine (4-Vpy), 4-*tert*-butylpyridine (4-*t*Bupy) and 4-phenylpyridine (4-Phpy)] were synthesized and characterized using spectroscopic and electrochemical techniques, as well as magnetic susceptibility to check the paramagnetism of these compounds. These complexes were tested as catalytic precursors in hydrogenation reactions with cyclohexene, undecanal and cyclohexanecarboxaldehyde, as compounds bearing C=C and C=O groups. Broad screening was carried out in order to find the optimal reaction conditions with the highest conversion. It was found that by using a ratio of Ru-catalyst/substrate = 1:530 at 80 °C and 15 bar of H_2 for 24 h, cyclohexene can be reduced. Hydrogenation of undecanal was possible using a Ru-catalyst/substrate ratio of 1:100 at 160 °C and 100 bar for 24 h, and for the reduction of cyclohexanecarboxaldehyde the reaction conditions were Ru-catalyst/substrate ratio of 1:100 at 160 °C and 50 bar for 24 h.

1. Introduction

The chemistry of ruthenium complexes is very attractive due to the wide range of applications of these compounds in electron transfer reactions [1], as homogeneous catalysts in numerous types of organic reactions [2–8], as thin films [9–12], as compounds with potential anti-Trypanosomal activity [13–17], antitumor [18–22], antiparasitic [14] and anti-tuberculosis [23,24].

The aqua-complex *mer*-[$RuCl_3$(dppb)(H_2O)] [25] is frequently used in our group due to its versatility as a precursor for the synthesis of various new [Ru_n-Cl_n(dppb)] containing compounds with different dimensionality, such as mononuclear, binuclear and supramolecular complexes [26–28]. The structural and electrochemical properties of this aqua-complex make it a unique compound to be used in different applications, such as a potential anticancer drug [29], electrochemical devices [30,31], and as catalysts in the hydrogenation of ketones [32].

Thus, having in mind that ruthenium complexes have been used as homogeneous catalysts for a series of alkene reactions, in this study we decided to synthesize and characterize some 6-coordinate, octahedral, *mer*-[$RuCl_3$(dppb)(N)] (N = pyridine and derivatives) complexes and to study their catalytic properties in hydrogenation reactions of cyclohexene, undecanal and cyclohexanecarboxaldehyde. Therefore, five Ru complexes with phosphine and pyridine based ligands, namely *mer*-[$RuCl_3$(dppb)(N)] [dppb = 1,4-bis(diphenylphosphino)butane and N = pyridine (py) **1**, 4-methylpyridine (4-Mepy) **2**, 4-vinylpyridine (4-Vpy) **3**, 4-*tert*-butylpyridine (4-*t*Bupy) **4** and 4-phenylpyridine (4-Phpy) **5**], were synthesized. The complexes with pyridine, 4-methylpyridine and 4-vinylpyridine were previously reported [26], but nothing is known about their catalytic properties. Pivotal catalytic parameters such as reaction time, catalyst concentration, gas pressure and

* Corresponding author.
** Corresponding author.
E-mail addresses: albogado@pontal.ufu.br (A.L. Bogado), daab@ufscar.br (A.A. Batista).
[1] In memoriam of Claudia Rodrigues.

http://dx.doi.org/10.1016/j.molstruc.2016.01.080
0022-2860/

temperature were studied in order to identify the optimal conditions for activity of the catalysts.

2. Experimental section

2.1. Materials and methods

2.1.1. Chemistry

Solvents were purified by standard methods. All chemicals used were of reagent grade or comparable purity. $RuCl_3 \cdot 3H_2O$, triphenylphosphine (PPh_3), 1,4-*bis*(diphenylphosphino)butane (dppb), pyridine (py), 4-methylpyridine (4-Mepy), 4-vinylpyridine (4-Vpy), 4-*tert*-butylpyridine (4-*t*Bupy) and 4-phenylpyridine (4-Phpy) were used as received from Aldrich. The precursors $[RuCl_2(PPh_3)_3]$, $[RuCl_2(dppb)(PPh_3)]$ and *mer*-$[RuCl_3(dppb)(H_2O)]$ were prepared according to the literature [25,33,34]. The *mer*-$[RuCl_3(dppb)(py)]$ **1**, *mer*-$[RuCl_3(dppb)(4\text{-}Mepy)]$ **2**, *mer*-$[RuCl_3(dppb)(4\text{-}Vpy)]$ **3**, *mer*-$[RuCl_3(dppb)(4\text{-}^tBupy)]$ **4** and *mer*-$[RuCl_3(dppb)(4\text{-}Phpy)]$ **5** complexes were prepared according to the modified procedures [26].

2.1.2. X-ray crystallography

Red crystals of *mer*-$[RuCl_3(dppb)(4\text{-}Phpy)]$ were grown by slow evaporation of a dichloromethane/*n*-hexane/diethyl ether solution (2:1:1) at room temperature. The data collection was performed using Mo-Kα radiation ($\lambda = 71.073$ pm) on a BRUKER APEX II Duo diffractometer. Data reduction and absorption correction were carried out with the Bruker SAINT package. The structure was solved with SHELXS97 using direct methods [35] and all non-hydrogen atoms were refined with anisotropic displacement parameters with SHELXL97 [36]. The hydrogen atoms were calculated at idealized positions using the riding model option of SHELXL97 [36]. See in supporting information Table 1S, the detailed information about the structure determination.

2.1.3. Catalytic studies

Hydrogenation reactions were performed in 25 and 75 mL stainless steel autoclaves equipped with an overhead magnetic stirrer, a pressure indicator and a thermocouple for temperature registration. The autoclaves were equipped with an electrical heating/cooling system to control the temperature inside the vessel. The hydrogenation active catalyst substrate/Ru-complex was prepared *in situ*, once the Ru-complexes used were pre-catalysts. The autoclave was charged with Ru-complex (0.013, 0.015 or 0.026 mmol), substrate (1.5 or 6.9 mmol), MeOH (20 or 6 mL). The system was flushed three times with H_2. Then, the autoclave was pressurized with H_2 (15, 50 or 100 bar) and heated to a temperature of 80 or 160 °C, for 15 or 24 h. After the reaction, the homogeneous reaction mixture was cooled down in an ice bath to room temperature, and the upper organic layer was analyzed by GC-FID and GC-MS.

2.1.4. Preparation of ruthenium (III) complexes

mer-[RuCl$_3$(dppb)(N)], N = 4-vinylpyridine (4-Vpy), 4-tert-butylpyridine (4-tBupy) and 4-phenylpyridine (4-Phpy): Ruthenium (III) complexes **3**, **4** and **5** were synthesized similar to described in the literature for the synthesis of the **1** and **2** [26], reacting an equimolar amount of N-heterocyclic ligands (0.153 mmol) with the *mer*-$[RuCl_3(dppb)(H_2O)]$ precursor (0.100 g, 0.153 mmol). The reaction mixture was refluxed and stirred for 6 h, under Ar atmosphere, in a Schlenk flask. The final pink solutions were concentrated to *ca.* 2 mL and 10 mL of *n*-hexane, previously degassed, were added in order to obtain pink precipitates. The solids were filtered off, well rinsed with *n*-hexane and diethyl ether and dried *in vacuum*.

mer-[RuCl$_3$(dppb)(4-Vpy)] **3** Yield: 90 mg (85%). Calc. for $C_{35}H_{35}NP_2Cl_3Ru$: C, 56.88; H, 4.77; N, 1.90%. Found: C, 57.10; H, 5.03; N, 1.94%. IR (KBr): 695 and 498 cm^{-1}, ν(C=Npy), 512 cm^{-1}, ν(Ru–P), 413 cm^{-1} ν(Ru–N), 335, 313 and 286 cm^{-1}, ν(Ru–Cl). UV–Vis (CH_2Cl_2): 528 (1248), 450 (800) and 349 (1125) M^{-1} cm^{-1}.

mer-[RuCl$_3$(dppb)(4-tBupy)] **4** Yield: 87 mg (83%). Calc. for $C_{37}H_{41}NP_2Cl_3Ru$: C, 57.78; H, 5.37; N, 1.82%. Found: C, 57.51; H, 5.43; N, 1.77%. IR (KBr): 694 and 500 cm^{-1}, ν(C=Npy), 514 cm^{-1}, ν(Ru–P), 416 cm^{-1}, ν(Ru–N), 336, 316 and 287 cm^{-1}, ν(Ru–Cl). UV–Vis (CH_2Cl_2): 530 (1860), 441 (1200) and 350 (1750) M^{-1} cm^{-1}.

mer-[RuCl$_3$(dppb)(4-Phpy)] **5** Yield: 89 mg (84%). Calc. for $C_{39}H_{37}NP_2Cl_3Ru$: C, 59.36; H, 4.73; N, 1.78%. Found: C, 59.66; H, 4.63; N, 1.77%. IR (KBr): 695 and 495 cm^{-1}, ν(C=Npy), 513 cm^{-1}, ν(Ru–P), 413 cm^{-1}, ν(Ru–N), 336, 313 and 290 cm^{-1}, ν(Ru–Cl). UV–Vis (CH_2Cl_2): 536 (1250), 449 (850) and 353 (1450) M^{-1} cm^{-1}.

2.1.5. Instrumentation

Elemental analyses were performed in a Fison EA 1108 model.

The FTIR spectra of the powder complexes were recorded from KBr pellets in the 4000–200 cm^{-1} range, in a Bomen–Michelson FT MB-102 instrument.

The UV–Vis spectra of the complexes, in dichloromethane solution, concentration of 1×10^{-3} mol L^{-1}, were recorded with a Hewlett Packard diode array – 8452 A.

The Electron Paramagnetic Resonance (EPR) spectra in the solid state was measured at 77 K using a Varian E-109 instrument operating at the X band frequency, within a rectangular cavity (E-248) fitted with a temperature controller. X-band (9.4 GHz) EPR spectra were recorded at 100 K on an EMX cw-spectrometer (Bruker) equipped with a liquid N_2 cryostat and a temperature controller with a modulation frequency of 100 kHz, a microwave power 6.3 mW and modulation amplitude of 5 G.

Cyclic voltammetry (CV) experiments of the complexes, in solution, were conducted in an electrochemical analyzer BAS model 100B Instrument. These experiments were carried out at room temperature in CH_2Cl_2 containing 0.10 mol L^{-1} Bu_4NClO_4 (TBAP) (Fluka Purum) as a support electrolyte using a one-compartment cell, where the working and auxiliary electrodes were stationary Pt foils, and the reference electrode was Ag/AgCl, 0.10 mol L^{-1} TBAP in CH_2Cl_2. Under these conditions ferrocene was oxidized at 0.43 V (Fc+/Fc).

All the NMR experiments were recorded on BRUKER DRX400 MHz equipment; in a BBO 5 mm probe at 298 K, using $CDCl_3$ (^1H) and CH_2Cl_2 ($^{31}P\{^1H\}$) as solvents, TMS for internal reference for ^1H.

GC analysis was run on a Shimadzu CLASS-VPTM instrument (50 m capillary column, carrier gas: 3 atm N_2 and FID detector).

3. Results and discussion

3.1. Characterization of complexes containing Ru(III)

IR spectra for all complexes show the typical band of coordinated phosphine 512–514 cm^{-1} ν(Ru–P) and pyridine ligands 413–421 cm^{-1} ν(Ru–N). Three bands were observed, from 336 to 286 cm^{-1} ν(Ru–Cl), suggesting a meridional (*mer*) arrangement of the chlorine ligands [37]. The electronic spectra of the complexes in CH_2Cl_2 solutions in the UV–Vis region, showed three characteristic bands. The bands near 530, 450, and 350 nm can be tentatively attributed to Cl→Ru, N→Ru and P→Ru, ligand-metal charge transfer (LMCT), respectively [25,26].

The presence of ruthenium(III) species was confirmed by magnetic susceptibility experiments and EPR measurements (see Fig. 1). The EPR spectra of **1**–**3** complexes measured in frozen dichloromethane solution are shown in Fig. 1. All these complexes show rhombic signals, typical for isolated Ru(III) ions in a rhombic environment [38,39]. The positions of the signals were reproduced

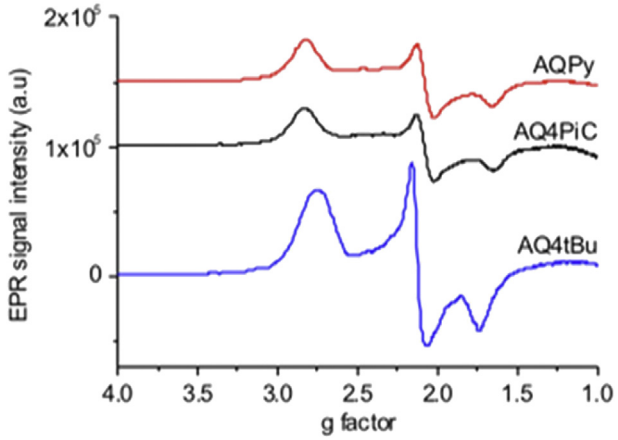

Fig. 1. EPR spectra of *mer*-[$RuCl_3$(dppb)(py)] **1** (AQPy), *mer*-[$RuCl_3$(dppb)(4-Mepy)] **2** (AQPic) and *mer*-[$RuCl_3$(dppb)(4-^{t}Bupy)] **3** (AQ4tBu) in frozen dichloromethane solution recorded at 100 K.

by simulating the corresponding experimental spectra [40] [AQPy = **1** (g_1 = 2.774, g_2 = 2.053 g_3 = 1.635), AQ4Pic = **2** (g_1 = 2.786, g_2 = 2.066 g_3 = 1.646), and AQ4tBu = **4** (g_1 = 2.71, g_2 = 2.093 g_3 = 1.716)] (see Fig. 1). These spectra are similar to those of *mer*-[$RuCl_3$(dppb)(py)] (g_1 = 2.928, g_2 = 2.037, g_3 = 1.607) and *mer*-[$RuCl_3$(dppb)(4-Mepy)] (g_1 = 2.487, g_2 = 2.101, g_3 = 1.866), previously reported in the literature [26]. The g-anisotropy of the Ru complexes increases in the order of AQPy < AQ4Pic < AQ4tBu, more probably due to the shape anisotropy imposed by the presence of different organic substituents in the pyridine ligand.

Cyclic voltammograms of the complexes, in CH_2Cl_2 solutions, at room temperature, reveal an irreversible Ru(III) → Ru(II) process (only one electron involved). In the first cycle, starting at 0.50 V, a reduction process was observed at −0.09 V (peak 1′) (See Fig. 2). In the second cycle, after inversion of the scan rate (at −0.40 V), two poorly defined oxidation processes were derived characterized by anodic peak potential (E_{pa}) at 0.52 V and 0.65 V, peaks 3 and 2, respectively. This electrochemical behavior can be explained considering that with the reduction of Ru III/II, at −0.07 to 0.03 V (in the first cycle), the species [Ru_2Cl_5(dppb)$_2$] (2), [Ru_2Cl_4(dppb)$_2$(L)] (3) and [$RuCl_2$(dppb)(L)$_2$] (4) should be generated on the electrode surface. In this case [Ru_2Cl_5(dppb)$_2$] (eq. 2), [Ru_2Cl_4(dppb)$_2$(N)] (eq. 3) and [$RuCl_2$(dppb)(N)$_2$] (eq. 4) complexes were generated, according to a suggested mechanism (see Scheme 1) (Table 1)[26].

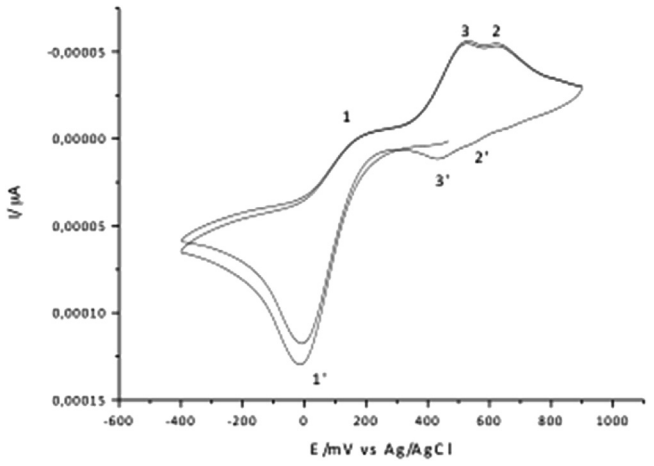

Fig. 2. Cyclic voltammograms of *mer*-[$RuCl_3$(dppb)(4-Phpy)] 5, 1.0 × 10^{-3} mol L^{-1}, for potentials between −400 and 1000 mV, *vs.* Ag/AgCl, recorded in CH_2Cl_2, in 0.1 mol L^{-1} TBAP; sweep rate 100 mV s^{-1}.

$$[RuCl_3(dppb)(N)] + e^- \rightarrow [RuCl_2(dppb)(N)] + Cl^- \text{ (eq. 1)}$$

$$[RuCl_3(dppb)(N)] + [RuCl_2(dppb)(N)] \rightarrow [Ru_2Cl_5(dppb)_2] + 2N \text{ (eq. 2)}$$

$$2[RuCl_2(dppb)(N)] \rightarrow [Ru_2Cl_4(dppb)_2(N)] + N \text{ (eq. 3)}$$

$$[RuCl_2(dppb)(N)] + N \rightarrow [RuCl_2(dppb)(N)_2] \text{ (eq. 4)}$$

Scheme 1. Redox mechanism of *mer*-[$RuCl_3$(dppb)(N)] complexes, where N = pyridine and derivatives.

Table 1
Redox potentials of cyclic voltammograms of *mer*-[$RuCl_3$(dppb) (N)] complexes (Ag/AgCl, 1.0 × 10^{-3} mol L^{-1}, 0.1 mol L^{-1} TBAP, CH_2Cl_2; sweep rate 100 mV s^{-1}).

Complexes	E_{pa} (V)			E_{pc}(V)		
	(1)	(3)	(2)	(1′)	(3′)	(2′)
1	0.15	0.50	0.60	−0.01	0.41	0.57
2	0.12	0.48	0.65	−0.07	0.42	0.58
3	0.12	0.42	0.54	−0.07	0.38	0.49
4	0.18	0.50	0.65	0.03	0.45	0.61
5	0.19	0.52	0.65	−0.09	0.45	0.59

E_{pa} = anodic peak potential, E_{pc} = cathodic peak potential. Labels of the studied complexes: *mer-[$RuCl_3$(dppb)(py)]* **1**, *mer-[$RuCl_3$(dppb)(4-Mepy)]* **2**, *mer-[$RuCl_3$(dppb)(4-Vpy)]* **3**, *mer-[$RuCl_3$(dppb)(4-tBupy)]* **4** and *mer-[$RuCl_3$(dppb)(4-Phpy)]* **5**.

An ORTEP representation of the molecular structure of *mer*-[$RuCl_3$(dppb)(4-Phpy)], as well as the numbering scheme are presented in Fig. 3. Selected bond lengths and angles for this compound are shown in the caption of Fig. 3. The crystal structure presents a 6-coordinated complex where the metal center is surrounded by two phosphorous atoms, P(1) and P(2) of the bidentate dppb ligand, the pyridine nitrogen atom N(1) of the 4-Phpy ligand and three monoanionic chloride ligands in *mer* configuration, similar to those found in *mer*-[$RuCl_3$(dppb)(4-Mepy)] [26]. After coordination, the N-heterocyclic ligand occupies the position that was previously occupied by H_2O in the precursor, *trans* positioned

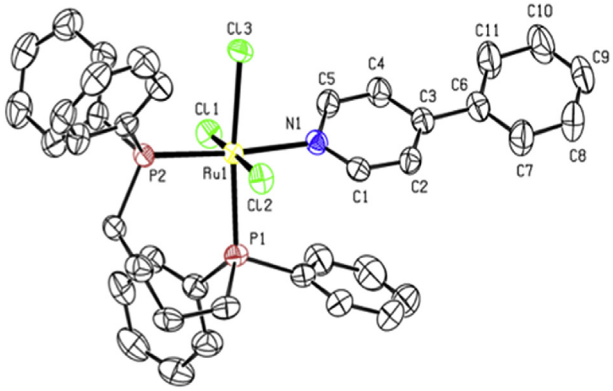

Fig. 3. Ellipsoid representation of the molecular structure of *mer*-[$RuCl_3$(dppb)(4-Phpy)], 50% of probability ellipsoids. Hydrogen atoms have been omitted for clarity. **Selected bond lengths [Å]**: Ru(1)-N(1) 2.1920(19), Ru(1)-Cl(1) 2.3304(6), Ru(1)-Cl(2) 2.3373(6), Ru(1)-Cl(3) 2.4056(6), Ru(1)-P(1) 2.4166(6), Ru(1)-P(2) 2.3438(6). **Selected Bond Angles [°]**: N(1)-Ru(1)-Cl(1) 88.26(5), N(1)-Ru(1)-Cl(2) 89.45(5), Cl(1)-Ru(1)-Cl(2) 175.50(2), N(1)-Ru(1)-P(2) 174.67(5), Cl(1)-Ru(1)-P(2) 91.73(2), Cl(2)-Ru(1)-P(2) 90.91(2), N(1)-Ru(1)-Cl(3) 82.54(5), Cl(3)-Ru(1)-P(1) 173.27(2), Cl(1)-Ru(1)-Cl(3) 90.86(2), Cl(2)-Ru(1)-Cl(3) 92.68(2), P(2)-Ru(1)-Cl(3) 92.13(2), N(1)-Ru(1)-P(1) 90.82(5), Cl(1)-Ru(1)-P(1) 87.84(2), Cl(2)-Ru(1)-P(1) 88.33(2), P(2)-Ru(1)-P(1) 94.50(2).

to the P(2) of the dppb ligand, while one chloride, Cl(3), is in *trans* position to the P(1) atom. The slightly longer Ru–P(1) distance (2.4166 Å) compared to the Ru–P(2) bond length (2.3438 Å) can be attributed to the better σ-donor properties of the chloride ligand, when compared with the pyridine ring from 4-phenylpyridine, *trans* to the P(2) atom. The Ru–Cl(3) bond distance (2.4046 Å) is longer than that of Ru–Cl(1) and Ru–Cl(2) (2.3304 and 2.3373 Å, respectively) due to the *trans* effect of the phosphorus atom, P(2). The angles Cl(1)-Ru(1)-Cl(2), N(1)-Ru(1)-P(2) and Cl(3)-Ru(1)-P(1), all around 174°, show a low distortion for the octahedral environment in the region of the ruthenium(III) metal center.

3.2. Catalytic activity in hydrogenation reactions

The catalytically active ruthenium species for hydrogenation reactions were *in situ* prepared by the reaction of the substrate with the Ru(III) precursor in the presence of molecular hydrogen. Scheme 2 describes the general conditions to obtain the hydrogenated products from cyclohexene (1c), undecanal (1b) and cyclohexanecarboxaldehyde(1c). In order to determine the best reaction conditions, a series of experiments was performed varying pressure, temperature and catalyst concentration. The results for these reactions are present in Table 2.

It is possible to observe in the Table 2 for the hydrogenation of cyclohexene (1a), that there is no substantial difference among the catalytic activity of the ruthenium complexes **1**–**5**. All complexes were active in the reaction conditions of 7.5 bar H_2, 80 °C, 150 rpm, 1:530 Ru-complex/(1a) and they showed a good performance with an average of 78.8% of the hydrogenated product. The reduction of the C=C in the cyclohexene was obtained with rates between 26 and 30 h^{-1} (*turnover frequency* - TOF) (see Table 2, entries from 1 to 5).

To better understand the influence of precursors on the catalytic activity, the solvent from the reaction with *mer*-[$RuCl_3$(dppb)(4-Vpy)] **3** was removed under vaccum and the isolated yellow powder was characterized by FTIR, conductivity and NMR spectroscopy.

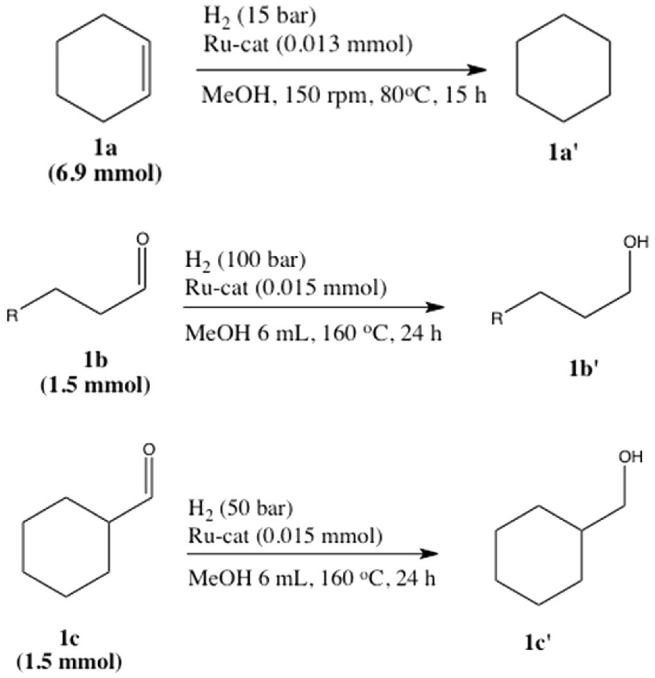

Scheme 2. Hydrogenation of cyclohexene (1a), undecanal (1b) and cyclohexanecarboxaldehyde (1c) with *mer*-[$RuCl_3$(dppb)(N)] complexes.

Table 2
Catalytic activity of the complexes containing Ru (III) in the hydrogenation of cyclohexene (1a), undecanal (1b) and cyclohexanecarboxaldehyde (1c).

Entry	Catalytic precursor	Substrate	Yields (%)	TOF (h^{-1})
1	*mer*-[$RuCl_3$(dppb)(py)][A]	1a	84	30
2	*mer*-[$RuCl_3$(dppb)(4-Mepy)][A]	1a	73	26
3	*mer*-[$RuCl_3$(dppb)(4-Vpy)][A]	1a	78	28
4	*mer*-[$RuCl_3$(dppb)(4-tBupy)][A]	1a	83	29
5	*mer*-[$RuCl_3$(dppb)(4-Phpy)][A]	1a	76	27
6	*mer*-[$RuCl_3$(dppb)(4-Vpy)][B]	1a	87	31
7	*mer*-[$RuCl_3$(dppb)(4-Vpy)][C]	1a	2	0.71
8	*mer*-[$RuCl_3$(dppb)(4-Vpy)][D]	1a	86	15
9	*mer*-[$RuCl_3$(dppb)(4-Vpy)][E]	1a	96	34
10	*mer*-[$RuCl_3$(dppb)(4-Vpy)][F]	1a	87	31
11	*mer*-[$RuCl_3$(dppb)(4-Vpy)][G]	1b	93	4
12	*mer*-[$RuCl_3$(dppb)(4-Vpy)][H]	1c	73	3

[A] reaction conditions: Ru-cat 0.013 mmol, H_2 pressure 7.5 bar, 20 mL of MeOH, mechanical stirring 150 rpm, 15 h, temperature 80 °C; [B] addition of 15 μL of triethylamine (NEt3); [C] addition of an excess (2:1) of ligand 4-Vpy; D using 0.026 mmol of catalyst; [E] using 15 bar H_2 pressure; [F] RT; [G] Ru-cat 0.015 mmol, H_2 pressure 100 bar, 6 mL of MeOH as solvent, mechanical stirring 150 rpm, 24 h reaction time, temperature 160 °C; [H] Ru-cat 0.015 mmol, H_2 pressure 50 bar, 6 mL of MeOH as solvent, mechanical stirring 150 rpm, 24 h reaction time, temperature 160 °C. TOF (h^{-1}) *turnover frequency* = $n_{pro}/(n_{cat} \times t)$; where n_{pro} = mols number of product, n_{cat} = mols number of catalyst and t = reaction time (h).

The FTIR (KBr, solid-state) showed a characteristic band due the ν(Ru–H) stretching at 1945 cm^{-1}, and the H^1 NMR ($CDCl_3$ solution) spectrum showed a broad sign at δ −2.42 ppm, attributed to η^2-H_2 molecule. When the complex contains a terminal hydride ligand in addition to a coordinated η^2-H_2 molecule, the terminal hydride is usually found at lower frequency, where the chemical shifts are usually in the range δ−5 to −45 ppm. The ^1H chemical shifts for the coordinated η^2-H_2 molecule are often found at low frequency with respect to TMS and can be relatively broad due to inter and intramolecular exchange dynamics [41]. Additionally it is also observed in the ^1H NMR data a chemical shift related to N–H bond at δ 11.48 ppm (supporting information, Fig. 1S). Therefore, it suggests the presence of the protonated 4-VpyH$^+$, and a cationic metal complex with formula [RuCl(η^2-H_2)(dppb)(cxe)$_2$]$^+$, obtained by chloride displacement {where cxe = cyclohexene}.

In towards of this view, the conductivity value of the 1.0×10^{-3} mol L^{-1} solution of *mer*-[$RuCl_3$(dppb)(4-Vpy)] is neutral, 1.60 μS cm^{-1}, in CH_2Cl_2 (1:1 electrolyte range 12–77 μS cm^{-1}), but the conductivity value in the same concentration of the residual solution after catalysis presented 1:1 conductivity value, 12.78 μS cm^{-1}, which is in agreement with the presence of the salts described above.

The ^{31}P {^1H} NMR ($CDCl_3$) of the residual complex showed a singlet signal at δ 34 ppm, due the magnetic equivalence of the P, and it corresponded with the formation of a kind of Ru(II), attributed to [RuCl(η^2-H_2)(dppb)(cxe)$_2$]$^+$ (supporting information, Fig. 2S). The dichloride complex *trans*-[$RuCl_2$(dppb)(cxe)$_2$] was synthesized from *mer*-[$RuCl_3$(dppb)(H_2O)] under H_2 atmosphere and an excess (3:1) of cyclohexene within 7 h. The yellow solution was reduced to *ca.* 2 mL, and dimethyl ether was added to precipitate the complex. A pale yellow solid was obtained quantitatively and it was filtered off by cannula filtration. The ^{31}P {^1H} NMR data showed a singlet at δ 37 ppm (supporting information, Fig. 3S), which is close to the chemical shift of the residual complex after the catalytic reaction, labeled as [RuCl(η^2-H_2)(dppb)(cxe)$_2$]$^+$.

This effort gives support to the similar catalytic behavior observed for the complex **1**–**5** in the hydrogenation of cyclohexene (entries from 1 to 5 in the Table 2), suggesting no dependence between N-groups coordinated to the metal center and the catalytic results. This attempt contributed to understand the drastic decrease in the catalytic performance when *mer*-[$RuCl_3$(dppb)(4-

Vpy)] was applied in the presence of an excess of free 4-Vpy (2:1) (entry 7, Table 2). The TOF was reduced to 0.71 h^{-1}, demonstrating the competition of the olefinic substrate with N-groups to the same site of coordination.

It is well know in the catalytic hydrogenation systems that the presence of triethylamine (NEt_3) can promote the release of halogenated ligands, such as chloride ions. However, the addition of 15 μL of NEt_3 (entry 6, Table 2), does not improve the activity of precursor as expected, only 87% of the hydrogenated product was obtained. This result is similar in absence of NEt_3 (entry 3, Table 2), where 78% of hydrogenated product was obtained. It is interesting to observe, that complex with general formula *mer*-[$RuCl_3$(dppb)(L)] {L = H_2O [25] or N-donor groups} has the Ru—Cl bond length *trans* to P atom longer than the others (see the caption of Fig. 3), which suggested a weaker bond with the metal center. In the presence of a chloride scavenger, such as NEt_3, the chloride ion could be released easier, to promote the $NEt_3H^+Cl^-$ salt. However, it does not improve the performance of the precursors **1**–**5** applied in the catalytic system. The release of chloride is a kinetic pathway, and it should improve the initial rates of the reaction, but after 15 h of reaction, it showed no improvement in the yields of the product. Comparing the reactions containing twofold catalyst concentration, 0.026 mmol (entry 8, Table 2) no advantage was observed in the yield. However, with the reaction using a twice hydrogen pressure higher, 15 bar (entry 9, Table 2), the quantitative amount of the product was obtained.

The hydrogenation of Undecanal (1b) resulted in the formation of undecanol (1b′) with 93% of yields. The screenings of H_2-pressure, temperature and catalyst concentration were conducted in order to identify optimal reaction conditions. The best results for this reaction were obtained at 100 bar H_2, 160 °C, 150 rpm and 1:100 Ru-complex/substrate (entry 11, Table 2). In the best case, the reduction of the C=O bond took place in 4 h^{-1}.

The hydrogenation product of cyclohexanecarboxaldehyde (1c) is cyclohexylmethanol (1c′) with 73% of yields. The best result for this reaction was obtained in the presence of 50 bar H_2, 160 °C, 150 rpm and a ratio of 1:100 Ru-complex/substrate (entry 12, Table 2). The reduction of the C=O (aldehyde group) was achieved at 3 h^{-1}.

4. Conclusions

The complexes with general formula *mer*-[$RuCl_3$(dppb)(N)] [where dppb = 1,4-bis(diphenylphosphino)butane and N = pyridine (py), 4-methylpyridine (4-Mepy), 4-vinylpyridine (4-Vpy), 4-*tert*-butylpyridine (4-*t*Bupy) and 4-phenylpyridine (4-Phpy)] were synthesized and characterized, and they were tested as catalytic precursor on the hydrogenation of cyclohexene. All five complexes are active in this kind of reaction, and they showed good conversion and acceptable TOF values. However, it was observed no dependence of N-donor groups coordinated to the metal center in the yields of the hydrogenated product, but the behavior of those complexes involves the activation of the precursor, owing to a reduction *in situ* of the complexes and the labilization of N-donor groups. The complex *mer*-[$RuCl_3$(dppb)(4-Vpy)] was applied also in the aldehyde hydrogenation, showed good conversion and acceptable TOF values.

Conflict of interest disclosure

The authors declare no competing financial interest.

Acknowledgment

The authors would like to acknowledge the financial support from CNPq, CAPES, FAPESP and FAPEMIG. They would also like to acknowledge the Leibniz-Institut für Katalyse an der Universität Rostock e.V., Germany, for the support of EPR analyses and aldehydes hydrogenation.

Appendix A. Supplementary data

Supplementary data related to this article can be found at http://dx.doi.org/10.1016/j.molstruc.2016.01.080.

References

[1] Ceccanti, P. Diversi, G. Ingrosso, F. Laschi, A. Lucherini, S. Magagna, P. Zanello, J. Organomet. Chem. 526 (1996) 251–262.
[2] M. Haukka, L. Alvila, T.A. Pakkanen, J. Mol. Catal. A Chem. 102 (1995) 79–92.
[3] J. Norinder, C. Rodrigues, A. Börner, J. Mol. Catal. A Chem. 391 (2014) 139–143.
[4] K.-I. Tominaga, Y. Sasaki, J. Mol. Catal. A Chem. 220 (2004) 159–165.
[5] B.R. James, F. Lorenzini, Coord. Chem. Rev. 254 (2010) 420–430.
[6] E.S.F. Ma, B.O. Patrick, B.R. James, Inorg. Chim. Acta 408 (2013) 126–130.
[7] J. Pospech, I. Fleischer, R. Franke, S. Buchholz, M. Beller, Angew. Chem. Int. 52 (2013) 2852–2872.
[8] B.R. James, Hydrogenation reactions catalyzed by transition metal complexes, in: F.G.A. Stone, W. Robert (Eds.), Adv. Organomet. Chem., Academic Press, 1979, pp. 319–405.
[9] Y. Murakami, J. Li, T. Shimoda, Mater. Lett. 152 (2015) 121–124.
[10] J. Pazinato, D.M. Hoffmeister, K.P. Naidek, E. Westphal, H. Gallardo, H. Winnischofer, Electrochim. Acta 153 (2015) 574–582.
[11] M.J. Bosiak, M. Rakowiecki, A. Wolan, J. Szlachta, E. Stanek, D. Cycoń, K. Skupień, Dyes Pigments 121 (2015) 79–87.
[12] R. Fernandes, N. Patel, R. Edla, N. Bazzanella, D.C. Kothari, A. Miotello, Appl. Catal. A General 495 (2015) 23–29.
[13] C.L. Donnici, M.H. Araújo, H.S. Oliveira, D.R.M. Moreira, V.R.A. Pereira, M. de Assis Souza, M.C.A.B. de Castro, A.C.L. Leite, Biorg. Med. Chem. 17 (2009) 5038–5043.
[14] M.I.F. Barbosa, R.S. Corrêa, K.M. de Oliveira, C. Rodrigues, J. Ellena, O.R. Nascimento, V.P.C. Rocha, F.R. Nonato, T.S. Macedo, J.M. Barbosa-Filho, M.B.P. Soares, A.A. Batista, J. Inorg. Biochem. 136 (2014) 33–39.
[15] L. Otero, G. Aguirre, L. Boiani, A. Denicola, C. Rigol, C. Olea-Azar, J.D. Maya, A. Morello, M. González, D. Gambino, H. Cerecetto, Eur. J. Med. Chem. 41 (2006) 1231–1239.
[16] L. Otero, P. Noblia, D. Gambino, H. Cerecetto, M. González, J.A. Ellena, O.E. Piro, Inorg. Chim. Acta 344 (2003) 85–94.
[17] C. Rodrigues, A.A. Batista, J. Ellena, E.E. Castellano, D. Benítez, H. Cerecetto, M. González, L.R. Teixeira, H. Beraldo, Eur. J. Med. Chem. 45 (2010) 2847–2853.
[18] W.H. Ang, A. Casini, G. Sava, P.J. Dyson, J. Organomet. Chem. 696 (2011) 989–998.
[19] R. Sáez, J. Lorenzo, M.J. Prieto, M. Font-Bardia, T. Calvet, N. Omeñaca, M. Vilaseca, V. Moreno, J. Inorg. Biochem. 136 (2014) 1–12.
[20] Z. Wang, H. Qian, S.-M. Yiu, J. Sun, G. Zhu, J. Inorg. Biochem. 131 (2014) 47–55.
[21] E. Tfouni, D.R. Truzzi, A. Tavares, A.J. Gomes, L.E. Figueiredo, D.W. Franco, Nitric Oxide 26 (2012) 38–53.
[22] T.A. Heinrich, G. Von Poelhsitz, R.I. Reis, E.E. Castellano, A. Neves, M. Lanznaster, S.P. Machado, A.A. Batista, C.M. Costa-Neto, Eur. J. Med. Chem. 46 (2011) 3616–3622.
[23] D. Cappoen, J. Vajs, C. Uythethofken, A. Virag, V. Mathys, M. Kofçevar, L. Verschaeve, M. Gazvoda, S. Polanc, K. Huygen, J. Košmrlj, Eur. J. Med. Chem. 77 (2014) 193–203.
[24] F.R. Pavan, G.V. Poelhsitz, M.I.F. Barbosa, S.R.A. Leite, A.A. Batista, J. Ellena, L.S. Sato, S.G. Franzblau, V. Moreno, D. Gambino, C.Q.F. Leite, Eur. J. Med. Chem. 46 (2011) 5099–5107.
[25] L.R. Dinelli, A.A. Batista, K. Wohnrath, M.P. de Araujo, S.L. Queiroz, M.R. Bonfadini, G. Oliva, O.R. Nascimento, P.W. Cyr, K.S. MacFarlane, B.R. James, Inorg. Chem. 38 (1999) 5341–5345.
[26] K. Wohnrath, M.P. de Araujo, L.R. Dinelli, A.A. Batista, I. de Sousa Moreira, E.E. Castellano, J. Ellena, J. Chem. Soc. Dalton Trans. (2000) 3383–3386.
[27] M.P. de Araujo, E.M.A. Valle, J. Ellena, E.E. Castellano, E.N. dos Santos, A.A. Batista, Polyhedron 23 (2004) 3163–3172.
[28] A.L.R. Silva, M.O. Santiago, I.C.N. Diógenes, S.O. Pinheiro, E.E. Castellano, J. Ellena, A.A. Batista, F.B. do Nascimento, Í.S. Moreira, Inorg. Chem. Commun. 8 (2005) 1154–1158.
[29] A.E. Graminha, C. Rodrigues, A.A. Batista, L.R. Teixeira, E.S. Fagundes, H. Beraldo, Spectrochim. Acta Part A Mol. Biomol. Spectrosc. 69 (2008) 1073–1076.
[30] C. Rodrigues, A.A. Batista, R.Q. Aucélio, L.R. Teixeira, L.D.C. Visentin, H. Beraldo, Polyhedron 27 (2008) 3061–3066.
[31] F.G. Delolo, C. Rodrigues, M.M.D. Silva, L.R. Dinelli, F.N. Delling, J. Zukerman-Schpector, A.A. Batista, J. Braz. Chem. Soc. 25 (2014) 540–549.
[32] M.P. de Araujo, A.T. de Figueiredo, A.L. Bogado, G. Von Poelhsitz, J. Ellena, E.E. Castellano, C.L. Donnici, J.V. Comasseto, A.A. Batista, Organometallics 24 (2005) 6159–6168.

[33] T.A. Stephenson, G. Wilkinson, J. Inorg. Nucl. Chem. 28 (1966) 945–956.
[34] C.W. Jung, P.E. Garrou, P.R. Hoffman, K.G. Caulton, Inorg. Chem. 23 (1984) 726–729.
[35] G.M. Sheldrick, SHELXS97-Program for the Solution of Crystal Structures, University of Göttingen, Germany, 1997.
[36] G.M. Sheldrick, SHELXL97-Program for the Refinement of Crystal Structures, University of Göttingen, Germany, 1997.
[37] K. Nakamoto, Infrared and Raman Spectra of Inorganic and Coordination Compounds, Wiley Inter-Science, Hoboken, NJ, USA, 1997.
[38] A.A. Batista, C. Pereira, K. Wohnrath, S.L. Queiroz, R.H. de A. Santos, M.T. do P. Gambardella, Polyhedron 18 (1999) 2079–2083.
[39] G. von Poelhsitz, M.P. de Araujo, L.A.A. de Oliveira, S.L. Queiroz, J. Ellena, E.E. Castellano, A.G. Ferreira, A.A. Batista, Polyhedron 21 (2002) 2221–2225.
[40] W.R. Hagen, Biomolecular EPR Spctroscopy, CRC Press, Boca Raton, FL, USA, 2009.
[41] P.S. Pregosin, NMR in Organometallic Chemistry, Wiley-VCH Verlag GmbH & Co. KGaA, Weinheim, Germany, 2012.